J|A|C|S
COMMUNICATIONS

Published on Web 09/18/2002

Anomalous Magnetic Properties of MnO Nanoclusters

Gang H. Lee,*,† Seung H. Huh,† Jin W. Jeong,† Byeong J. Choi,† Seung H. Kim,† and Hyeong-C. Ri‡

Department of Chemistry, College of Natural Sciences, Kyungpook National University, Taegu 702-701, South Korea, and Material Science Laboratory, Korea Basic Science Institute, 52 Yeoeun-Dong, Yusung-Ku, Taejeon 305-333, South Korea

Received July 3, 2002

The nanoclusters of metal oxides have been a great interest because they have shown a ferromagnetic behavior even though they are antiferromagnetic in the bulk phase.[1−7] In the same way, MnO nanoclusters are predicted to be ferromagnetic by theory[1] even though their bulk phase is antiferromagnetic.[8,9] In this communication, we experimentally report, for the first time, that MnO nanoclusters with cluster diameters of 5−10 nm show a ferromagnetic behavior with a phase transition from ferromagnetic to paramagnetic phases at 27 K. We observed large coercivities up to 9500 Oe and a remanence of 1.72 emu/g at 2 K, which are typically observed values for ferromagnetic materials. Although it is not clear, this abnormal ferromagnetic behavior of MnO nanoclusters may arise from particle size effects.

The similar unusual magnetic behavior in several other metallic oxide nanoclusters such as NiO[4−7] and MnO(OH)[2] nanoclusters had been observed by other researchers. Nayak and Jena recently calculated magnetic properties of $(MnO)_{n=1-9}$ molecular clusters and obtained unusually high magnetic moments of 4−5 μ_B per MnO molecule.[1] Kodama et al. also observed large coercivities and large magnetic moments in NiO nanoclusters.[4] They, by using a multisublattice model, speculated that the unexpected high magnetic moments of NiO nanoclusters might be related to reduced coordination of surface spins which eventually induced the change in the magnetic order throughout the nanoclusters.

MnO nanoclusters were synthesized by thermally decomposing $Mn_2(CO)_8$ vapors with a resistive heater. The details regarding the experimental setup had been described elsewhere.[10] Briefly, about 1−2 mg of $Mn_2(CO)_8$ sample was loaded into the reaction chamber. The reaction chamber was heated to 200 °C to vaporize the solid $Mn_2(CO)_8$ sample. The $Mn_2(CO)_8$ vapors were then thermally decomposed by using a resistive heater made of Nichrome wire at a temperature of 400−450 °C. The reaction was completed in a few minutes. The final product was black and was kept in a vacuum until it was characterized by using an X-ray diffraction (XRD) spectrometer with Cu Kα radiation of 0.15418 nm (Philips, model: X-PERT), a transmission electron microscope (TEM) operating at an acceleration voltage of 300 keV (JEOL, model: JEM 3010), and a magnetic property measurement system (MPMS) (Quantum Design, model: MPMS 7).

Figure 1 represents an XRD pattern which shows that MnO nanoclusters have the same face-centered-cubic (fcc) structure as the bulk phase. The lattice constant was determined to be $a = 0.4427$ nm, which is consistent with the bulk value.[11] The two tiny peaks below the (111) peak in the XRD pattern (i.e., $2\theta = 29.0°$ (112) and 32.4° (103)) seem to arise from tetragonal γ-Mn_2O_3 nanoclusters with lattice constants of $a = 0.57$ and $c = 0.94$ nm,

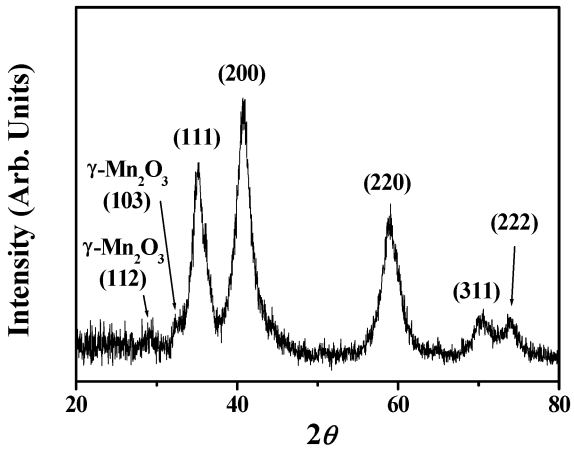

Figure 1. XRD pattern of MnO nanoclusters. The structure corresponds to a fcc structure. The two tiny peaks before the (111) peak originate from tetragonal γ-Mn_2O_3 nanoclusters. The assignments are the Miller indices (*hkl*).

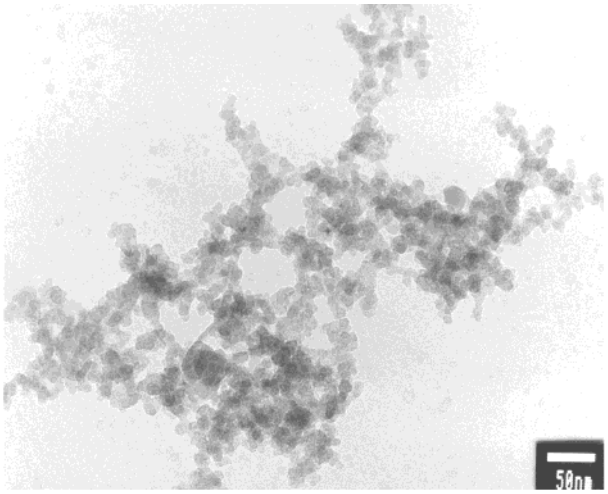

Figure 2. TEM micrograph of MnO nanoclusters taken at an acceleration voltage of 300 keV.

as is consistent with the bulk values.[12] With the measured full-width at half-maximums (fwhms) of the peaks[13] and Scherrer's formula,[14] the average cluster diameter was estimated to be 4.2 nm, which is well consistent with the roughly estimated value of 5−10 nm from the TEM micrograph (Figure 2). Here, the individual cluster diameter in the TEM micrograph is not clearly visible due to aggregation between MnO nanoclusters.

The magnetic properties were characterized by recording both magnetization curves as a function of temperature (Figure 3) and hysteresis loops at various temperatures (Figure 4). The zero field

* To whom correspondence should be addressed. E-mail: ghlee@bh.knu.ac.kr.
† Kyungpook National University.
‡ Korea Basic Science Institute.

10.1021/ja027558m CCC: $22.00

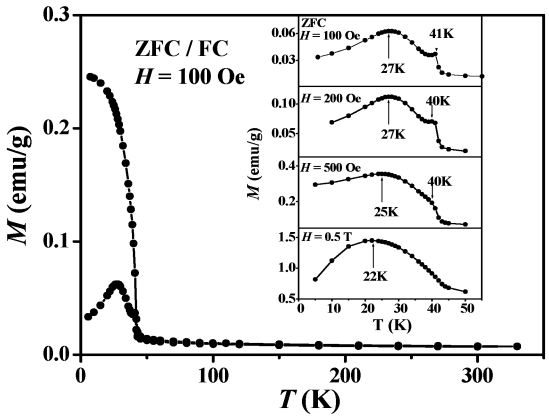

Figure 3. Magnetization curve of MnO nanoclusters versus temperature at an applied field of 100 Oe. Inserted are the short-range scans at applied fields of 100, 200, 500, and 5000 Oe.

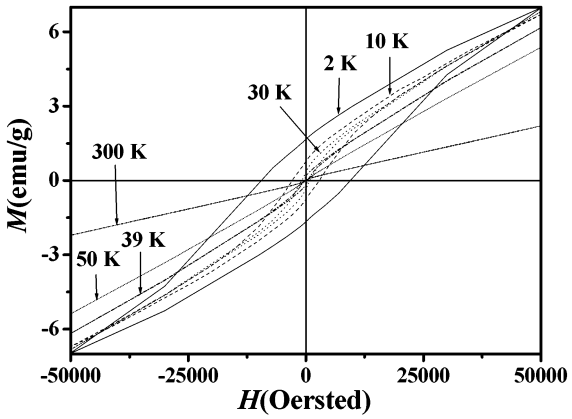

Figure 4. Hysteresis loops of MnO nanoclusters at 2, 10, 30, 39, 50, and 300 K.

cooled (ZFC)/field cooled (FC) magnetization curves at an applied field (H) of 100 as well as the ZFC magnetization curves at applied fields of 100, 200, 500, and 5000 Oe (i.e., the inserted figures in Figure 3) clearly show that there exists a phase transition from ferromagnetic to paramagnetic phases at the corresponding low temperatures (T_c) of 27, 27, 25, and 22 K, respectively. The hysteresis loops recorded at lower temperatures than T_c (i.e., at 2 and 10 K) show large coercivities and large remanences, which are typically observed values for ferromagnetic materials. The temperature dependences of both coercivity and remanence are represented in Figure 5, showing nearly zero values for both coercivity and remanence above $T = 50$ K, confirming paramagnetism above this temperature, as is consistent with the magnetization curve. Here, it seems that there exists another phase transition from ferromagnetic to paramagnetic phases around 40−41 K, as is indicated in the inserted figures in Figure 3. Although it is not clear, this phase transition may be due to γ-Mn_2O_3 nanoclusters existing as tiny impurities in the sample because the two tiny peaks from γ-Mn_2O_3 nanoclusters were observed in the XRD pattern (Figure 1), implying that γ-Mn_2O_3 nanoclusters are also ferromagnetic at a low temperature as are MnO nanoclusters.

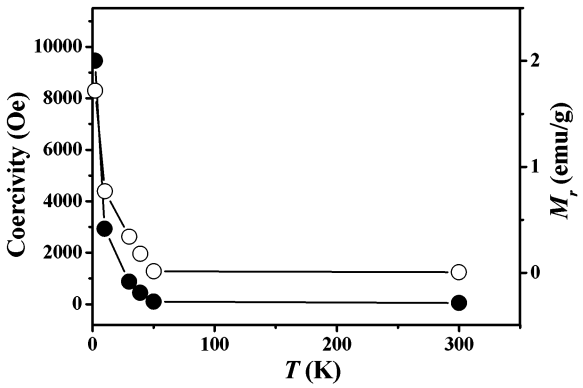

Figure 5. Coercivity (●) and remanence (M_r, ○) of MnO nanoclusters versus temperature.

The ferromagnetic behavior of MnO nanoclusters is not clearly understood. However, one possibility for this ferromagnetism may be related to cluster size effects or surface spin effects. For nanoclusters, the surface-to-volume ratio is very large, and surface atoms possess reduced coordination, which may alter spin configurations throughout the nanoclusters. To more clearly understand this ferromagnetic behavior, however, more extended works via either experiments (for instance, the measurement of magnetic properties as a function of cluster diameter, ranging from 0.5 to 50 nm, which may allow us to know about cluster size dependence and, thus, cluster size effects of ferromagnetic properties of MnO nanoclusters) or theoretical calculations will be necessary.

Acknowledgment. This work was supported by KOSEF-ABRL (2002) and Daegu City 2002 Nano Project. We would like to thank the Korea Basic Science Institute (KBSI) for allowing us to use their XRD at a membership rate and also thank the material science group at KBSI for allowing us to use their MPMS through a cooperational research project.

References

(1) Nayak, S. K.; Jena, P. *J. Am. Chem. Soc*. **1999**, *121*, 644.
(2) Li, J.; Wang, Y. J.; Zou, B. S.; Wu, X. C.; Lin, J. G.; Guo, L.; Li, Q. S. *Appl. Phys. Lett*. **1997**, *70*, 3047.
(3) Zhiwen, C.; Shuyuan, Z.; Shun, T.; Fanqing, L.; Jian, W.; Sizhao, J.; Yuheng, Z. *J. Cryst. Growth* **1997**, *180*, 280.
(4) Kodama, R. H.; Makhlouf, S. A.; Berkowitz, A. E. *Phys. Rev. Lett*. **1997**, *79*, 1393.
(5) Richardson, J. T.; Yiagas, D. I.; Turk, B.; Forster, K. *J. Appl. Phys*. **1991**, *70*, 6977.
(6) Schuele, W. J.; Deetscreek, V. D. *J. Appl. Phys*. **1962**, *33*, 1136.
(7) Richardson, J. T.; Milligan, W. O. *Phys. Rev*. **1956**, *102*, 1289.
(8) Neubeck, W.; Ranno, L.; Hunt, M. B.; Vettier, C.; Givord, D. *Appl. Surf. Sci*. **1999**, *138*, 195.
(9) Towler, M. D.; Allan, N. L.; Harrison, N. M.; Saunders, V. R.; Mackrodt, W. C.; Aprà, E. *Phys. Rev. B* **1994**, *50*, 5041.
(10) Huh, S. H.; Oh, S. J.; Kim, Y. N.; Lee, G. H. *Rev. Sci. Instrum*. **1999**, *70*, 4366.
(11) Moore, T. E.; Ellis, M.; Selwood, P. W. *J. Am. Chem. Soc*. **1950**, *72*, 856.
(12) Gui, Z.; Fan, R.; Chen, X.-H.; Wu, Y.-C. *Inorg. Chem. Commun*. **2001**, *4*, 294.
(13) The peaks used for calculation of average diameter: (*hkl*) (fwhm, 2θ) = (111) (1.74°, 35.20°); (200) (2.06°, 40.82°); (220) (2.43°, 59.05°). The Cu Kα line of 0.15418 nm was used as a radiation source.
(14) Cullity, B. D. *Elements of X-ray Diffraction*; Addison-Wesley: Reading, 1978; p 102.

JA027558M